Volume 12, No.8, August 2025

Journal of Global Research in Mathematical Archives

ISSN 2320 – 5822

RESEARCH PAPER

Available online at http://www.jgrma.com

IDENTIFICATION OF BRAIN TUMOR IN MRI LEVERAGING MULTI-SCALE ATTENTION ARCHITECTURE BASED ON EFFICIENTNETB4

Dr. Bal Krishna Sharma[1]

[1] Professor, Department of Computer Sciences and Applications, Mandsaur University, Mandsaur
bksharma7426@gmail.com

Abstract: It takes a long time to diagnose brain tumors (BT), and radiologists must possess a high degree of skill and expertise. The amount of data that has to be handled has increased along with the number of patients, rendering earlier methods both expensive and inefficient. A state-of-the-art approach for brain cancer detection and MRI segmentation is presented in this work by utilizing the EfficientNetB4 DL architecture. The principal data source is the Figshare Brain Tumor Dataset, which contains 3064 contrast-enhanced T1-weighted MRI slices from tumors within the pituitary, meningioma, and glioma areas. To increase the quality of the images and the performance of the models, extensive preprocessing methods were used, such as image scaling, min-max normalization, CLAHE, and Gaussian blur. Better results have been obtained using the EfficientNetB4 model with 80:20 data splits, with accuracy of 99.7%, F1-score 93.6%, recall 91.0%, precision 96.5%, and dice score 93.3%. A comparison with cutting-edge models such as UNet, VNet, and SVM showed how much better the suggested model was in segmentation accuracy and resilience. Through automated MRI image processing, findings demonstrate EfficientNetB4's potential to facilitate precise and effective brain tumor detection.

Keywords: Brain Tumor Diagnosis, MRI, Deep Learning, Image Segmentation, Glioma, Meningioma, Pituitary Tumor, Automated Detection, Medical Image Analysis.

1. INTRODUCTION

Healthcare systems across the globe are increasingly dependent on technological advancements to decrease human error, increase diagnostic precision, and enhance patient outcomes [1]. Early and precise detection of life-threatening conditions such as cancer is a critical component of modern healthcare, enabling timely intervention and improved prognosis. Among all forms of cancer, tumors abnormal growths of tissue resulting from uncontrolled cellular division represent a significant cause of morbidity and mortality [2][3]. These can impair organ function and may become fatal if not diagnosed and treated promptly. The brain controls almost every aspect of human life, from perception and emotion to thinking and language [4][5]. It is an incredibly intricate and important organ. The frontal lobe is represented by the number one in Figure 1, the parietal lobe by numbers 5 and 6, the occipital lobe by number 7, and the temporal lobe by number 8. The human brain's primary areas for processing information are located here [6][7][8]. In addition to reasoning, emotions, and decision-making, the frontal lobe is in charge of speech and motor abilities. The parietal lobe processes touch and spatial information.

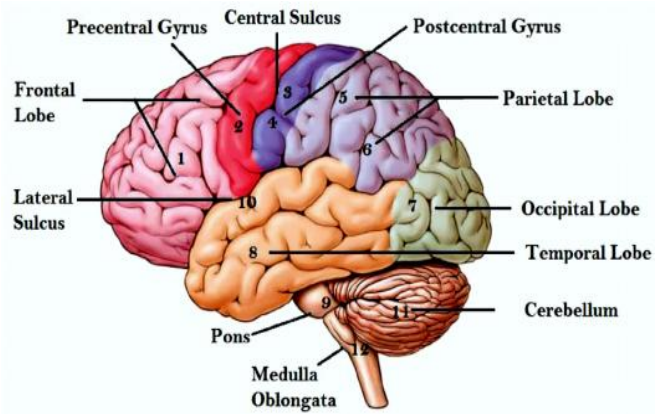

Figure 1: Major functional areas of human brain

Brain tumors, a subset of central nervous system (CNS) diseases, are particularly critical due to the brain's primary function in controlling essential body processes. As a result of the proliferation of abnormal cells within the brain, a brain tumor can either begin in the brain itself or spread to other parts of the body, a process known as metastasis [9][10][11]. The malignant variety of these tumors is more aggressive, invasive, and prone to recurrence than the benign variety, which falls into the lower grade category. The most prevalent and lethal kind of primary brain tumor among the several kinds is glioma, which frequently needs prompt and intense treatment.

Finding the best treatment approaches requires accurate brain tumor diagnosis and classification [12][13]. Brain tumors are best detected via magnetic resonance imaging (MRI), which is considered the clinical gold standard due to its non-invasiveness and enhanced contrast in soft tissues. MRI offers anatomical high-resolution images to identify the tumors during their initial stages and their effect on the surrounding brain structures [14][15][16]. However, reading of MRI images is usually based on expertise of the radiologists and thus labor-intensive, time-consuming, and subjective [17]. There is an urgent need to develop automated systems that could help clinicians identify and segment brain tumors with high accuracy and precision since the need of efficient and consistent medical imaging analysis is increasing.

The use of artificial intelligence (AI) in brain tumor diagnostics and early detection, and thus, it is potent in complementing the brain tumor surgery, which is an infamous task. Smaller artificial intelligence applications such as machine learning (ML) and deep learning (DL) have transformed neuropathology work, especially in medical image processing, and have created new opportunities to create intelligently designed diagnostic instruments [18][19]. DL-based models can detect minor patterns that cannot be identified by the human eye, which makes them perfect in the analysis of brain tumors.

1.1 Motivation and Contribution of the Study

High-resolution Medical image processing continues to face significant challenges in MRI image segmentation and categorization of brain tumors, especially gliomas, because of their complex forms, which exhibit size and location variability, and great resemblance to healthy brain tissue. Radiologists are unable to give consistent diagnosis and treatment planning when interpreting MRI data by hand since it is subjective, time-consuming, and vendor-dependent. The current research is inspired by the pressing necessity of the development of an automated, reliable and precise diagnostic tool, that could help clinicians in early and correct diagnosis of brain tumors. The proposed framework is set to solve the current limitations in medical images segmentation by incorporating innovative DL methods, including the EfficientNetB4 model of architecture. It is also motivated by the growing incidence and mortality of gliomas, which require intelligent solutions that can support the development of personalized treatment planning by differentiating low-grade and high-grade gliomas accurately, and eventually, it can lead to better clinical outcomes and more optimized healthcare provision. The following are this work's main contributions:

- To have confident input during model training and evaluation, got and prepared a brain tumor MRI dataset of Figshare repository Kaggle.
- To improve picture quality and model input, preprocessing methods such image scaling, normalization, CLAHE, and Gaussian blur were used and optimized.
- Applied the DL architecture, which has the capability of being both computationally efficient and accurate, to classify brain tumor regions, in this case, EfficientNet B4.
- The results are presented in their whole because the model's performance was evaluated using multiple credible metrics, such as the F1-score, accuracy, recall, precision, and Dice similarity coefficient.
- Demonstrated the efficiency of the suggested method in reliably automating the identification and segmentation of brain tumors, supporting its applicability in clinical decision-making.

1.2 Novelty and Justification of the Study

The novelty of this study lies in the integration of advanced image preprocessing techniques with the EfficientNet B4 architecture to enhance brain tumor segmentation accuracy in MRI scans. Unlike traditional models or manual methods, this approach combines contrast enhancement (CLAHE) and noise reduction (Gaussian blur) to improve input image quality, thereby enabling the DL model to learn more discriminative features. EfficientNet B4, known for its optimized balance between accuracy and computational efficiency, offers superior performance compared to conventional CNNs. The justification for this study is rooted in the growing demand for precise, automated diagnostic tools in neuroimaging that can assist clinicians in early detection and reduce the workload associated with manual tumor annotation. This study offers a reliable and scalable method suited to practical clinical applications, furthering the continuous development of AI-driven medical imaging.

1.3 Structure of the Paper

The following is the paper's outline: Begin with a literature review on brain tumor detection on MRI scans utilizing Figshare data in Section 2. The technique is outlined in Section 3. Results and model comparisons are shown in Section 4. Finally, insights and future research possibilities are offered in Section 5.

2. LITERATURE REVIEW

This section reviews current developments in the use of MRI images to classify brain tumors, emphasizing the use of DL, hybrid models, and transfer learning approaches to improve processing speed and diagnostic accuracy.

Singla and Gupta (2025) presented a DL approach for MRI image-based brain tumor categorization, leveraging the Xception architecture for efficient and accurate detection. The dataset consisted of images related to brain tumors and healthy ones. The model was preprocessed and image enhancement was used to improve its performance. The network that was fine-tuned with transfer learning resulted in a test accuracy of about 98.9% with minor loss, indicating its good discriminative capability between the case of brain tumor and the healthy one. Evaluation of the performance by confusion matrix analysis indicates high sensitivity and specificity levels with just minor false positives and false negatives [20].

Ridwan et al. (2025) presented an innovative method to identify and classify brain tumors successfully. Their system, formulated for MRI scans, uses techniques such as CNN, Vision Transformer, Transfer Learning, and hybrid model to detect and identify three specific types of tumors: pituitary, glioma, and meningioma. They trained their DL models using well-organized sets of tumor and non-tumor MRI images. The accuracy of Vision Transformer is 99.08%, while the Hybrid CNN-ViT got 98.05% The Transfer Learning with VGG16 showed an accuracy of 97.08% Also, when they put together the EfficientNet, ResNet, and VGG models, they achieved accuracy rates of 94.11%, 94.75%, and 94.96%, respectively [21].

B, G S and V (2025) provided an innovative DL framework for classifying MRI images of brain tumors into four groups: those involving the pituitary gland, meningiomas, gliomas, and those without disease. A collection of 7,022 MRI scans from several archives, such as Figshare, SARTAJ, and Br35H, was used, a novel framework is proposed by implementing a multi-task classification strategy using CNNs alongside Xception Learning to detect tumors, classify them based on malignancy and type, and identify their locations within the brain. The suggested framework has a training accuracy of 98.13% and training loss of 0.1675. Comparatively, the validation and test accuracies were 95.11 and 93.60 respectively with precision and recall measures being much higher than 90% in most of the classes with confusion matrices indicating high classification powers [22].

Sharma and Mittal (2024) offered a novel hybrid DL model with the goal of improving performance in brain tumor classification. During the feature extraction procedure, the model makes advantage of the VGG19 model's features, LSTM to learn the correlations in time, and SVM to make a correct classification. The dataset is made up of 7023 MRI pictures that were taken from three non-repetitive datasets—Figshare, SARTAJ, and Br35H—for training and testing. One significant improvement the remedying of misclassification within the glioma category, by substituting mislabeled SARTAJ photos with those having the correct labeling in Figshare. The F1-score, the recall, the accuracy, and the precision are some of the metrics used to evaluate the performance of the suggested model. A potent tool for the detection and diagnosis of brain tumors, the model's classifications have a 97% accuracy rate [23].

Nizamli and Filatov (2024) presented a tweaked version of the transfer learning algorithm that aims to produce state-of-the-art functionality that employs MRI scans to categories various brain tumor types. The pre-trained VGG-19 is developed with fixed weights and constitutes, in the suggested method, a mapping of the MRI scans onto a high-level numerical representation. The traits are then fed into an SVM algorithm, which separates brain tumors into three main groups: pituitary, meningioma, and glioma. The effectiveness of using feature optimization techniques using radial basis similarity and L1-penalty LR was investigated in order to improve the model's performance even more. As an assessment tool, the benchmark dataset Fig share that comprises 3064 MRI images was applied following a sequence of operations. Compared to other analogues, the high overall accuracy of 98.53% was reached in the proposed system [24].

Chowdhury and Kibria (2023) medical industry can greatly benefit from the suggested systems. According to the current study, a CNN was used to experimentally extract brain tumours from 2D Magnetic Resonance Imaging (MRI) data. These MRI scans would be used in the suggested strategy to develop the best model for distinguishing between various types of brain malignancies, including pituitary tumours, and normal brain structures, meningiomas, and gliomas. Network architecture, hyperparameter choice, and optimisation method complexity all affect how well a model performs. CNN, which used for the study, has a very high accuracy score of 98.91% [25].

Sahoo, Parida and Muralibabu (2023) study investigated the feasibility of utilising k-means and CLA clustering techniques on MRI data for the purpose of tumour classification in the brain. The dataset used in the study was sourced from the Figshare website and included 3064 T1-CE MRI scans of three distinct types of cancer: meningioma, glioma, and pituitary. As the dice similarity and accuracy factors are applied, respectively, they are found to be 99.47% and 83.37% using the K-means clustering technique. The dice similarity coefficient and accuracy, as determined by CLA clustering, are 86.65% and 99.64%, respectively [26].

Bohra and Gupta (2022) A brain tumor is a potentially fatal disorder that interferes with the brain's natural processes. Brain tumors must be identified early for a conclusive diagnosis and an effective active treatment strategy. The categorization of a brain tumor is based on the expertise and experience of the doctor. However, for quick examination of brain tumors, an independent method is required. This study included three feature extraction methods: Inception v3, VGG16, and VGG19. Following the identification of the features, ML classifiers are used to differentiate between brain tumors that are malignant (cancerous) and benign (non-cancerous). When utilizing the logistic regression classifier and VGG16, the findings yield the best accuracy of 97.7% [27].

The comparative analysis of background study based on their Methodology, Dataset/Environment, Problem Addressed, Performance and Future Work/Limitation is provided in Table 1.

Table 1: Related summary on Brain Tumor Detection on MRI Scans

Author	Dataset Used	Algorithm / Model Used	Performance Achieved	Limitations/Gap
Singla and Gupta (2025)	Brain tumor vs. healthy MRI images (unspecified source)	Xception with transfer learning	Test Accuracy: 98.9%, High sensitivity & specificity	Focused only on binary classification (tumor vs. no tumor); lacks tumor type segmentation
Ridwan et al. (2025)	MRI dataset for pituitary, glioma, and meningioma	CNN, Vision Transformer, VGG16,	ViT: 99.08%, CNN-ViT: 98.05%, VGG16: 97.08%,	Multi-model comparison lacks integration into a unified

		Hybrid CNN-ViT, ResNet, EfficientNet	ResNet: 94.75%, EfficientNet: 94.11%	framework; segmentation component not emphasized
B, G S and V (2025)	7022 MRI images (Figshare, SARTAJ, Br35H)	Multi-task CNN with Xception Learning	Training Accuracy: 98.13%, Validation: 95.11%, Testing: 93.60%, Precision/Recall > 90%	Relatively lower test accuracy; lacks robust generalization for unseen datasets
Sharma and Mittal (2024)	7023 MRI images (Figshare, SARTAJ, Br35H)	Hybrid model: VGG19 + LSTM + SVM	Classification Accuracy: 97%	Temporal features (LSTM) may not add significant value for static MRI images; complexity increases training time
Nizamli and Filatov (2024)	Figshare (3064 MRI images)	VGG-19 + SVM with radial basis function and L1-penalty logistic regression	Accuracy: 98.53%	Feature extraction fixed (non-trainable); lacks end-to-end deep learning adaptability
Chowdhury and Kibria (2023)	Real-time online dataset with different tumor intensities, sizes, and forms	Custom CNN model	Accuracy: 98.91%	Dataset details not well-defined; lacks benchmarking with transfer learning or hybrid models
Sahoo et al. (2023)	Figshare (3064 T1-CE MRI scans)	K-Means Clustering vs. CLA Clustering	CLA Accuracy: 99.64%, Dice Score: 86.65%	Unsupervised clustering may struggle with multi-class differentiation; lacks CNN or DL-based comparative baseline
Bohra and Gupta (2022)	Not specified explicitly	Feature extraction (VGG16, VGG19, Inception v3) + ML classifiers (e.g., Logistic Regression)	Accuracy: 97.7% (VGG16 + Logistic Regression)	Focused on classification only (not segmentation); limited interpretability and localization of tumor regions

3. METHODOLOGY

Medical diagnosis and treatment planning rely on brain cancer segmentation in MRI, which involves accurately identifying and classifying tumor areas. To obtain accurate diagnosis and treatment planning, the initial stage in the MRI brain tumor segmentation procedure is to collect figshare brain tumor data from Kaggle. Data preparation processes such as normalization, picture scaling, Contrast Limited Adaptive Histogram Equalization (CLAHE), and Gaussian blur are applied to the gathered dataset. Data sets used for training and testing are segregated following preprocessing. The EfficientNet B4 model for classification is then trained and assessed using the processed pictures. Evaluation parameters such as the F1-score, recall, accuracy, precision, and dice similarity coefficient are utilized to evaluate the model's performance, allowing for a comprehensive analysis of the segmentation and classification outcomes. The workflow for MRI scans to diagnose brain tumors is shown in Figure 2.

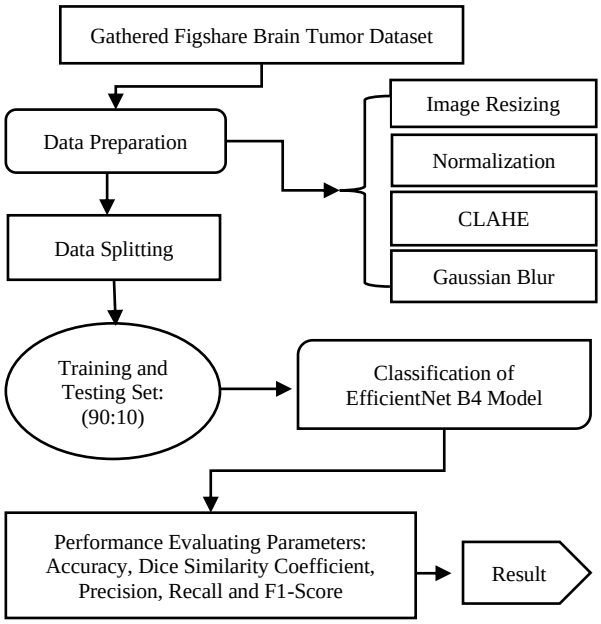

Figure 2: Flowchart of Brain Tumor Detection on MRI Scans

Each step of the flowchart is explained in the section below:

3.1 Data Collection

This study leverages Figshare Brain Tumor Dataset that is collected from Kaggle. In Figure 3, on the right, it can see the 3064 T1-weighted contrast-enhanced pictures of 233 individuals diagnosed with three different kinds of brain cancer: glioma (1,426 slices), meningioma (708 slices), and pituitary tumor (930 slices). Owing to the file size constraint imposed by the repository, the complete dataset was separated into four smaller groups. Each of the four subsets was included in 766 slices within a zip file. The 5-fold cross-validation indices are also provided. Below are some EDA graphs and heatmap of the dataset are displayed below:

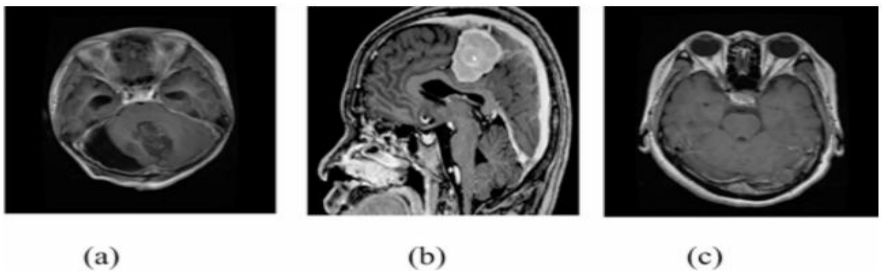

Figure 3. Sample of Figshare dataset. (a) Glioma. (b) Meningioma. (c) Pituitary tumor

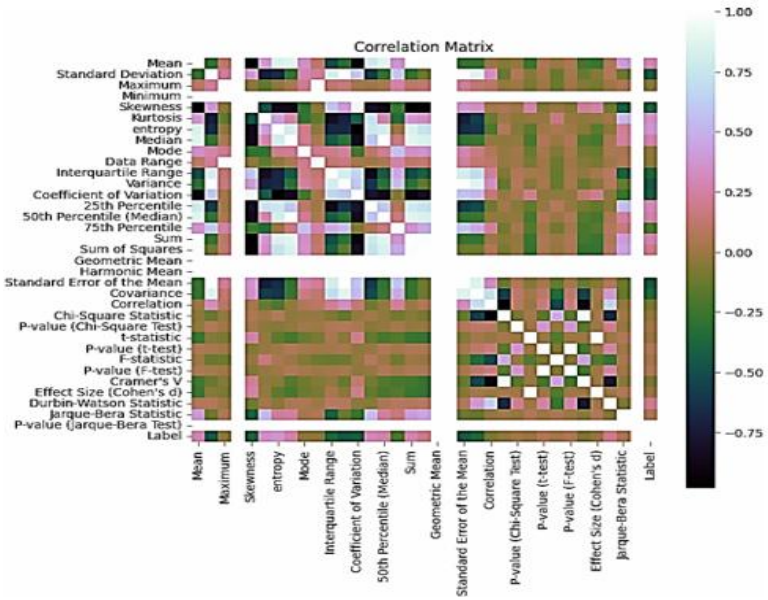

Figure 4. Heatmap of the Correlation matrix

Figure 4 presents a correlation matrix heatmap illustrating the pairwise relationships between statistical features and the 'Label' variable. The color scale ranges from dark black (strong negative correlation, -1.00) to bright cyan (strong positive correlation, 1.00), with green-brown tones indicating weak or no correlation. White diagonal elements represent perfect self-correlation. The matrix is symmetric, and distinct blocks reveal areas of strong or weak correlation, highlighting key features potentially relevant to the 'Label' variable.

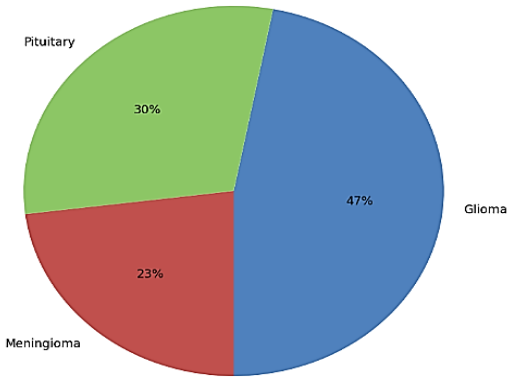

Figure 5. Data Distribution

The distribution of three different Brain tumor types includes meningioma, pituitary, and glioma is seen in Figure 5. The largest proportion, accounting for 47%, is attributed to Glioma, represented by the blue segment. Pituitary tumors constitute 30% of the

distribution, shown in green. The smallest share belongs to Meningioma, making up 23%, depicted by the red segment. The chart clearly visualizes the relative prevalence of these three tumor types within the dataset or population it represents.

3.2 Data Preprocessing

The main objective of purpose of pre-processing is to make MR pictures more readable and to transform them into a format that ML and humans can both use. Smoothing the interior of rooms, keeping their borders, removing extraneous items and background noise, and raising the signal-to-noise ratio, Pre-processing significantly improves MR images' visual quality. Therefore, this study employed image resizing, min-max normalization, CLAHE and Gaussian blur preprocessing steps that are discussed below:

- **Image Resizing:** The EfficientNetB4 design requires that all photos be scaled to a set size of 224 × 224 pixels [28]. This phase guarantees that the model processes pictures effectively and without distortion, uniformizes input size, and lowers computing loads.
- **Normalization:** Model fitting and learning functions are both affected by scale bias, therefore standardization and normalization work by adjusting variables evaluated at different scales. Model fitting is often preceded by feature-wise normalization, such Minmax Scaling. Each feature or variable in the input variables is given a range from 0 to 1, with a minimum value of 1, and a maximum value of 0, according to the minmax scaling transformation. Here is the mathematical expression for minmax scaling Equation (1):

$$x_{scaled} = \frac{x - \min(x)}{\max(x) - \min(x)} \quad (1)$$

- **CLAHE:** The area of interest (ROI), which is extracted once the tumor has been isolated, removes extraneous background in order for the model to standardize input dimensions and focus entirely on important features [29]. This method helps bring out fine features in the picture by redistributing brightness, which improves the contrast of the tumor area. Clip limit = 2.0 and grid size = (8 × 8) are employed by CLAHE to reduce inter-image variability brought on by variations in patient anatomy, MRI scanner settings, or lighting conditions in order to detect cancer spots.
- **Gaussian Blur:** MRI scans frequently have noise or artefacts from the acquisition process, which might mask important tumor characteristics. While maintaining the boundaries and specifics required for categorization, median filtering minimizes random noise without warping crucial features like tumor shapes [30]. The purpose of blurring is to remove non-tumor-related fluctuations and smooth out the picture at high frequencies. It helps reduce irrelevant data and encourages the model to ignore background noise and concentrate on the local characteristics of tumors.

3.3 Data Splitting

In training and testing, data splitting is the process of dividing a dataset into several subsets. 90% of the data used in this research paper's study was used as a training set, while 10% was used as an assessment set. This is referred to as the 90-10 data split.

3.4 EfficientNet B4 Model

EfficientNet is a series of CNN architectures that have achieved new efficiency and accuracy records in the image classification task. These models were constructed in a manner that is called compound scaling, Its scaling factors are employed to uniformly scale the resolution, depth, and breadth of a network [31]. This method can be used to perform better using fewer resources than conventional scaling techniques.

The architecture of EfficientNet-B4 is more extensive and profound than those of its predecessors. It is tailored to high-precision tasks, and therefore it is suitable for difficult tasks in such domains as medical image classification. The compound scaling method depends on EfficientNetB4 to determine a set of compound coefficients of depth, width, and image resolution, the key to maximizing the performance of the network [32]. Such an optimization problem is expressed mathematically as shown in Equation (2):

$$max_{d,w,r} Accuracy\big(N(d,w,r)\big) \quad (2)$$

Where d, w, r are scaling coefficients of network depth, width and resolution of the image respectively, $N(d,w,r)$ is the model of classification and $max_{d,w,r} Accuracy$ is the maximum accuracy of the model.

3.5 Performance Matrix

The trained models were assessed using various metrics, such as the f1-score, recall, accuracy, precision, and DSC [33]. Additional adjustments were made to boost performance based on the assessment results. When a dataset is fed into the model, it can detect TP, TN, FP, and FN, or false positives and negatives. TP stands for tumor occurrences that the model has successfully detected and labelled, whereas FP stands for non-tumor instances that have been mistakenly classified as tumors. Undiscovered tumors (FN) are ones that were overlooked during the course of the diagnostic procedure. TN is an acronym for genuine negatives that were precisely as was predicted. Below are the equations of the respective matrices:

3.5.1. Accuracy

The accuracy of the model is demonstrated by the percentage of MRI scans that are correctly predicted out of all forecasts. To determine the precision, it applies Equation (3):

$$\text{Accuracy} = \frac{\text{TP+TN}}{(\text{TP+TN+FP+FN})} \quad (3)$$

3.5.2. Dice Similarity Coefficient (DSC)

DSC calculates a critical statistic: The gap between the expected segmentation (P) and the ground truth (G). To accurately locate tumors, define boundaries, and schedule treatments, Models for segmentation with high DSC scores are employed. A score of 1 on the DSC is used for perfect overlap. It is described in Equation (4):

$$DSC = \frac{2|P \cap G|}{|P|+|G|} \quad (4)$$

Where: 2|P⋂G| is the overlapped pixel count between the predicted and ground truth sections, and |P| is the total pixel count in both the ground truth and predicted segmentations.

3.5.3. Precision

Precision evaluates how many of the MRI scans predicted as having a tumor actually have a tumor. The precision is calculated in Equation (5):

$$Precision = \frac{TP}{(TP+FP)} \quad (5)$$

3.5.4. Recall

Techniques for recalling the model's capacity to recognize actual tumor cases, or the percentage of accurately detected genuine tumors. The recall is mathematically depicted in Equation (6):

$$Recall = \frac{TP}{(TP+FN)} \quad (6)$$

3.5.5. F1-Score

The harmonic mean of memory and accuracy is used to find the F1-score, which is the middle score between the two. Equation (7) is used to figure out the F1-score:

$$F_1 - Score = 2 \times \frac{Precision \times Recall}{Precision+Recall} \quad (7)$$

3.5.6. Loss Function

A loss function is a mathematical measure of the discrepancy during training between the actual labels and the model's predictions.

4. RESULTS AND DISCUSSION

Windows 11 Pro, 32 GB of RAM, an NVIDIA GeForce RTX 3070 Ti GPU, a 12th Gen Intel® CoreTM i7-12700 CPU operating at 2.10 GHz, and a high-performance computing environment were all utilized for the implementation. The EfficientNetB4 model's segmentation performance for brain tumor diagnosis using the Figshare dataset is shown in Table 2. The model demonstrates outstanding accuracy, achieving 99.7%. Strong segmentation quality is shown by the Dice Score calculates how much the predicted and ground truth segmentations overlap, which is 93.3%. The model also has a high precision of 96.5% and recalls of 91.0%. The model's impressive performance in brain tumor segmentation tasks is supported by an F1-score of 93.6% and balanced precision and recall.

Table 2: Segmentation Performance of the EfficientNetB4 Model for Brain Tumor Detection on Figshare Dataset

Metrics	EfficientNetB4
Accuracy	99.7
Dice Score	93.3
Precision	96.5
Recall	91.0
F1-Score	93.6

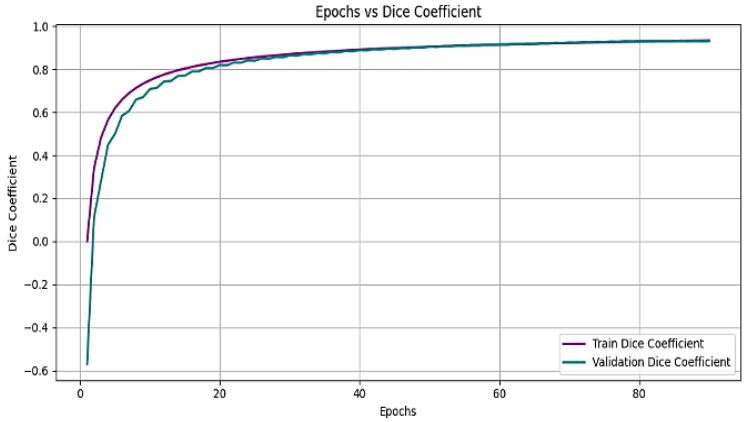

Figure 6: Dice Coefficient vs Epochs

Figure 6 shows how well the models with 80 epochs performed. The x-axis represents 80 epochs, while the y-axis represents the dice coefficient (-0.6 to 1.0). The purple line is Train Dice Coefficient and the teal line is the Validation Dice Coefficient. The two curves exponentially increase at the beginning albeit the training outcome is marginally higher. At an epoch of 80, they settle down to a score of about 0.9, which means that they are learning intensely with low levels of overfitting and equally performing on training and validation sets.

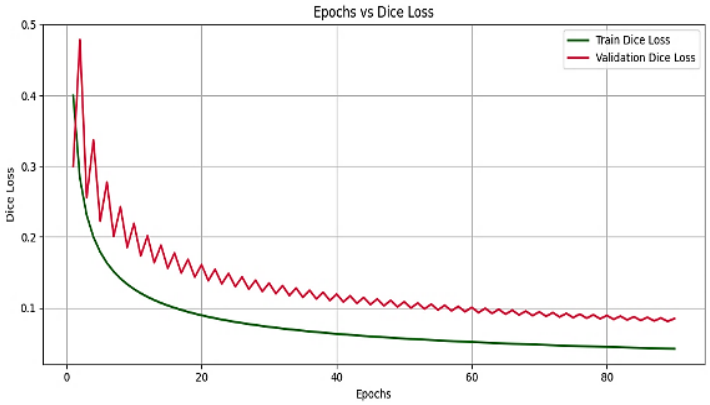

Figure 7. Dice Loss vs. Epochs

Figure 7 shows the Train and Validation Dice Loss over ~85 epochs. Epochs are represented by the x-axis, while dice loss (0.0 to 0.5) is displayed on the y-axis. The dark green line (train loss) decreases smoothly, while the red line (validation loss) follows a similar trend with some early fluctuations. Effective learning and strong generalization are indicated by both losses stabilizing at low values.

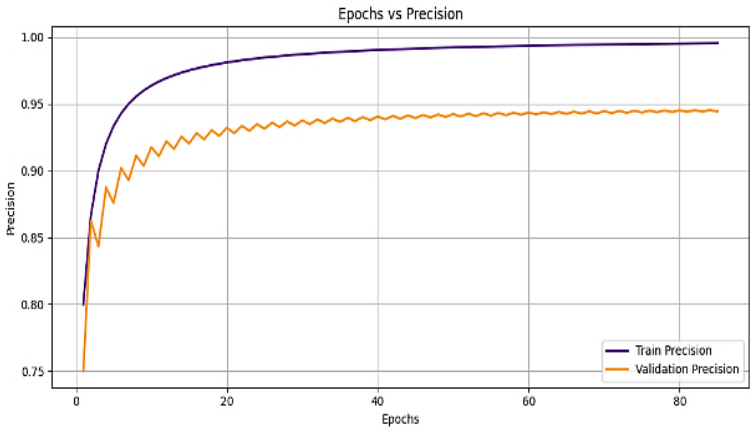

Figure 8. Precision vs. Epochs

The accuracy of training and validation during around 85 epochs is displayed in Figure 8. Precision is represented by the y-axis, which ranges from 0.75 to 1.00, while epochs are represented by the x-axis. The dark purple line indicates train precision, and the orange line shows validation precision. Both curves exhibit an upward trend, with train precision increasing sharply and stabilizing near 1.00 by 40–50 epochs. Validation precision also rises but with early fluctuations, stabilizing around 0.95 after 50 epochs. This indicates effective learning with slight performance variation on validation data.

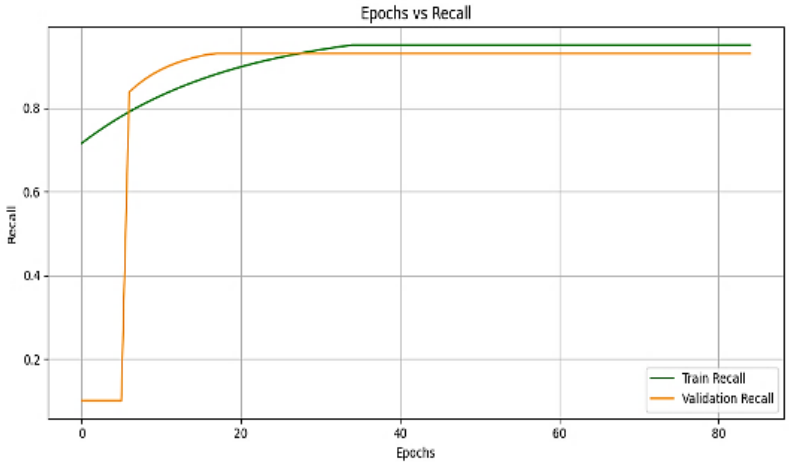

Figure 9. Recall vs. Epochs

The training and validation recall of a model across 85 epochs is displayed in Figure 9. The y-axis shows recall, which ranges from 0.0 to 1.0, while the x-axis shows 80 epochs. The green line (train recall) shows a steady rise from around 0.7 to a plateau near 0.95. The orange line (validation recall) starts low at 0.1, sharply increases after a few epochs, and gradually converges to a similar value near 0.95. Both curves stabilize at high recall values, indicating effective generalization and strong ability to identify relevant instances.

4.1 Comparative Analysis

Table 3 uses Accuracy and Dice Similarity Coefficient (DSC) metrics to assess the segmentation performance of many models for MRI scan-based brain tumor diagnosis. The traditional UNet architecture achieved an accuracy of 66.74% and a DSC of 80.23%, while VNet demonstrated superior performance with an 81.0% accuracy and an 88.0% DSC. The SVM-based approach, recorded a moderate accuracy of 74%. Notably, the EfficientNetB4 model outperformed all other methods with a significantly higher accuracy of 99.7% and a DSC of 93.3%, indicating its enhanced capability in accurately segmenting brain tumor regions and affirming its potential for clinical deployment in diagnostic imaging.

Table 3: Comparative Analysis of Segmentation Performance for Brain Tumor Detection Using MRI Scans

Models	Accuracy	Dice Similarity Coefficient
UNet [34]	66.74	80.23
VNet [35]	81.0	88.0
SVM [36]	74	-
EfficientNetB4	99.7	93.3

The suggested model, which uses the EfficientNetB4 framework, has shown excellent results in the use of MRI images for brain tumor segmentation, providing a precise and excellent result of tumor boundaries. It has the merits of high-level feature extraction, cost-effective computational resource and strong generalization in variable imaging conditions. Through compound scaling and the extensive architecture of the network, the model achieves the same level of computation efficiency as the segmentation quality improvement. The strengths also make it very appropriate to apply it in clinical workflows to provide a quick and accurate diagnosis of brain tumor using automation thus leading to better treatment planning and outcomes.

5. CONCLUSION AND FUTURE SCOPE

Early detection of brain cancer can really help to make sure that more people are not dying all around the globe. The shape, the sizes, and the structure of the tumor make the proper diagnosis of brain tumors quite challenging. Patients with brain tumors must consider the clinical implications of MR image categorization when making decisions about their treatment and clinical diagnosis. The MR images and tumor segmentation technique appear to be a desirable technique in identifying brain tumors early in their development. This study illustrates that deep CNN and innovative image-preprocessing methods might be used to successfully segregate brain tumors in MRI data. The framework designed significantly reduces manual segmentation thereby doing away with human error and boosting efficiency of diagnosis. The results underline the potential of the AI in developing the sphere of medical diagnostics and development of trustworthy, automated systems of tumor recognition and identification.

Further development will be aimed at increasing the current model to assist in multi-class tumor classification, and distinguishing between different types of tumors. Additionally, the integration of 3D volumetric MRI data is proposed to improve spatial context and segmentation precision. Further enhancements may include the incorporation of attention mechanisms or hybrid deep learning architectures to boost feature learning and accuracy. Real-time model deployment and extensive validation on diverse, large-scale clinical datasets will also be pursued to facilitate practical implementation in healthcare environments, ultimately aiming to support timely and effective patient care.

REFERENCES

[1] M. Rizwan, A. Shabbir, A. R. Javed, M. Shabbir, T. Baker, and D. Al-Jumeily Obe, "Brain Tumor and Glioma Grade Classification Using Gaussian Convolutional Neural Network," *IEEE Access*, vol. 10, pp. 1–10, 2022, doi: 10.1109/ACCESS.2022.3153108.

[2] A. Hossain *et al.*, "Brain Tumor Segmentation and Classification from Sensor-Based Portable Microwave Brain Imaging System Using Lightweight Deep Learning Models," *Biosensors*, vol. 13, no. 3, 2023, doi: 10.3390/bios13030302.

[3] S. Singamsetty, "Healthcare IoT Security: Examining Security Challenges and Solutions in the Internet of Medical Things. A Bibliometric Perspective," *J. Popul. Ther. Clin. Pharmacol.*, vol. 31, no. 8, pp. 1761–1806, Aug. 2024, doi: 10.53555/7j8dhs24.

[4] V. K. Singh, D. Pathak, and P. Gupta, "Integrating Artificial Intelligence and Machine Learning into Healthcare ERP Systems: A Framework for Oracle Cloud and Beyond," *ESP J. Eng. Technol. Adv.*, vol. 3, no. 2, pp. 171–178, 2023, doi: 10.56472/25832646/JETA-V3I6P114.

[5] R. Dattangire, D. Biradar, and A. Joon, "AI-Enhanced U-Net for Accurate Low-Grade Glioma Segmentation in Brain MRI: Transforming Healthcare Imaging," in *2024 Third International Conference on Electrical, Electronics, Information and Communication Technologies (ICEEICT)*, IEEE, Jul. 2024, pp. 1–6. doi: 10.1109/ICEEICT61591.2024.10718440.

[6] G. S. Tandel, A. Tiwari, O. G. Kakde, N. Gupta, L. Saba, and J. S. Suri, "Role of Ensemble Deep Learning for Brain Tumor Classification in Multiple Magnetic Resonance Imaging Sequence Data," *Diagnostics*, vol. 13, no. 3, 2023, doi: 10.3390/diagnostics13030481.

[7] R. P. Mahajan, "Transfer Learning for MRI image reconstruction: Enhancing model performance with pretrained networks," *Int. J. Sci. Res. Arch.*, vol. 15, no. 1, pp. 298–309, Apr. 2025, doi: 10.30574/ijsra.2025.15.1.0939.

[8] S. Pandya, "Predicting Diabetes Mellitus in Healthcare: A Comparative Analysis of Machine Learning Algorithms," *Int. J. Curr. Eng. Technol.*, vol. 13, no. 06, 2023, doi: 10.14741/ijcet/v.13.6.5.

[9] S. Khanmohammadi, M. Mobarakabadi, and F. Mohebi, "The Economic Burden of Malignant Brain Tumors," in *Advances in Experimental Medicine and Biology*, 2023. doi: 10.1007/978-3-031-14732-6_13.

[10] P. P. Jalaja, D. Kommineni, A. Mishra, R. Tumati, C. A. Joseph, and R. V. S. S. B. Rupavath, "Predictors of Mortality in Acute Myocardial Infarction: Insights From the Healthcare Cost and Utilization Project (HCUP) Nationwide Readmission Database," *Cureus*, vol. 17, no. 5, May 2025, doi: 10.7759/cureus.83675.

[11] S. R. Sagili, S. Chidambaranathan, N. Nallametti, H. M. Bodele, L. Raja, and P. G. Gayathri, "NeuroPCA: Enhancing Alzheimer's disorder Disease Detection through Optimized Feature Reduction and Machine Learning," in *2024 Third International Conference on Electrical, Electronics, Information and Communication Technologies (ICEEICT)*, IEEE, Jul. 2024, pp. 1–9. doi: 10.1109/ICEEICT61591.2024.10718628.

[12] M. A. Mostafiz, "Machine Learning for Early Cancer Detection and Classification: AIBased Medical Imaging Analysis in Healthcare," *Int. J. Curr. Eng. Technol.*, vol. 15, no. 03, pp. 1–10, 2025.

[13] B. K. R. Janumpally, "Securehealth: Edge-Enhanced Federated Architecture with Zero-Trust Framework for Privacy-Preserved Patient Monitoring," *Int. J. Comput. Eng. Technol.*, vol. 16, no. 1, pp. 1690–1705, 2025.

[14] M. De Simone, G. Iaconetta, G. Palermo, A. Fiorindi, K. Schaller, and L. De Maria, "Clustering Functional Magnetic Resonance Imaging Time Series in Glioblastoma Characterization: A Review of the Evolution, Applications, and Potentials," *Brain Sciences*. 2024. doi: 10.3390/brainsci14030296.

[15] S. Singamsetty, "Lightweight Reg Net-Driven Deep Learning Framework for Enhanced Classification of Neurodegenerative Diseases from MRI Images," *Int. J. Adv. Eng. Sci. Res.*, vol. 10, no. 1, pp. 28–37, 2023.

[16] R. P. Mahajan, "Optimizing Pneumonia Identification in Chest X-Rays Using Deep Learning Pre-Trained Architecture for Image Reconstruction in Medical Imaging," *Int. J. Adv. Res. Sci. Commun. Technol.*, vol. 5, no. 1, pp. 52–63, Apr. 2025, doi: 10.48175/IJARSCT-24808.

[17] S. Pandya, "Predictive Modeling for Cancer Detection Based on Machine Learning Algorithms and AI in the Healthcare Sector," *TIJER – Int. Res. J.*, vol. 11, no. 12, 2024.

[18] Y. Cao and Y. Song, "New Approach for Brain Tumor Segmentation Based on Gabor Convolution and Attention Mechanism," *Appl. Sci.*, vol. 14, no. 11, 2024, doi: 10.3390/app14114919.

[19] S. B. Shah, "Artificial Intelligence (AI) for Brain Tumor Detection: Automating MRI Image Analysis for Enhanced Accuracy," *Int. J. Curr. Eng. Technol.*, vol. 14, no. 06, Dec. 2024, doi: 10.14741/ijcet/v.14.5.5.

[20] S. Singla and R. Gupta, "Leveraging Transfer Learning and Image Processing for Brain Tumor Classification from MRI Data," in *2025 3rd International Conference on Advancement in Computation & Computer Technologies (InCACCT)*, 2025, pp. 134–138. doi: 10.1109/InCACCT65424.2025.11011464.

[21] M. Ridwan, T. T. Ali, S. T. T. Erin, R. K. Tushar, F. Mahmud, and S. Siddique, "MRI-Based Brain Tumor Detection and Classification System Using Vision Transformers and Transfer Learning," in *2025 IEEE International Conference on Interdisciplinary Approaches in Technology and Management for Social Innovation (IATMSI)*, 2025, pp. 1–6. doi: 10.1109/IATMSI64286.2025.10984625.

[22] S. B, A. Gandhi, and N. V, "A Novel Deep Learning Framework Utilizing Xception and CNNs for Enhancing Diagnostic

Accuracy in the Precise Classification of Brain Tumors from MRI Scans," in *2025 International Conference on Data Science, Agents & Artificial Intelligence (ICDSAAI)*, 2025, pp. 1–6. doi: 10.1109/ICDSAAI65575.2025.11011849.

[23] A. Sharma and S. Mittal, "Hybrid Deep Learning Model for Enhanced Brain Tumor Classification Using VGG19, LSTM, and SVM Algorithms," in *2024 Global Conference on Communications and Information Technologies (GCCIT)*, 2024, pp. 1–5. doi: 10.1109/GCCIT63234.2024.10862813.

[24] Y. A. Nizamli and A. Y. Filatov, "Improving Transfer Learning Performance for Abnormality Detection in Brain MRI Images Using Feature Optimization Techniques," in *2024 XXVII International Conference on Soft Computing and Measurements (SCM)*, 2024, pp. 432–435. doi: 10.1109/SCM62608.2024.10554161.

[25] M. J. U. Chowdhury and S. Kibria, "Performance Analysis for Convolutional Neural Network Architectures using Brain Tumor Datasets: A Proposed System," in *2023 International Workshop on Artificial Intelligence and Image Processing (IWAIIP)*, 2023, pp. 195–199. doi: 10.1109/IWAIIP58158.2023.10462886.

[26] A. K. Sahoo, P. Parida, and K. Muralibabu, "Effective Use of Clustering Techniques for Brain Tumor Segmentation," in *2023 IEEE 3rd International Conference on Applied Electromagnetics, Signal Processing, & Communication (AESPC)*, 2023, pp. 1–5. doi: 10.1109/AESPC59761.2023.10390467.

[27] M. Bohra and S. Gupta, "Pre-trained CNN Models and Machine Learning Techniques for Brain Tumor Analysis," in *2022 2nd International Conference on Emerging Frontiers in Electrical and Electronic Technologies, ICEFEET 2022*, 2022. doi: 10.1109/ICEFEET51821.2022.9847840.

[28] S. A. Pahune, "How does AI help in Rural Development in Healthcare Domain: A Short Survey," *Int. J. Res. Appl. Sci. Eng. Technol.*, vol. 11, no. VI, pp. 4184–4191, 2023.

[29] A. W. Setiawan, T. R. Mengko, O. S. Santoso, and A. B. Suksmono, "Color retinal image enhancement using CLAHE," in *Proceedings - International Conference on ICT for Smart Society 2013: "Think Ecosystem Act Convergence", ICISS 2013*, 2013. doi: 10.1109/ICTSS.2013.6588092.

[30] M. A. Rahman, M. B. A. Miah, M. A. Hossain, and A. S. M. S. Hosen, "Enhanced Brain Tumor Classification Using MobileNetV2: A Comprehensive Preprocessing and Fine-Tuning Approach," *BioMedInformatics*, vol. 5, no. 2, 2025, doi: 10.3390/biomedinformatics5020030.

[31] M. M. Islam, M. A. Talukder, M. A. Uddin, A. Akhter, and M. Khalid, "BrainNet: Precision Brain Tumor Classification with Optimized EfficientNet Architecture," *Int. J. Intell. Syst.*, vol. 2024, no. 1, p. 3583612, 2024, doi: https://doi.org/10.1155/2024/3583612.

[32] A. Mishra, "AI-Powered Cybersecurity Framework for Secure Data Transmission in IoT Network," *Int. J. Adv. Eng. Manag.*, vol. 7, no. 3, pp. 05–13, 2025.

[33] M. Ashimgaliyev, B. Matkarimov, A. Barlybayev, R. Y. M. Li, and A. Zhumadillayeva, "Accurate MRI-Based Brain Tumor Diagnosis: Integrating Segmentation and Deep Learning Approaches," *Appl. Sci.*, vol. 14, no. 16, 2024, doi: 10.3390/app14167281.

[34] A. K. Mandusia, "Brain Tumor Segmentation using Deep Learning-Based MRI Analysis," vol. 13, no. 08, pp. 108–112, 2024.

[35] K. Avazov, S. Mirzakhalilov, S. Umirzakova, A. Abdusalomov, and Y. I. Cho, "Dynamic Focus on Tumor Boundaries : A Lightweight U-Net for MRI Brain Tumor Segmentation," pp. 1–20, 2024.

[36] S. Akter, M. S. H. Talukder, S. K. Mondal, M. Aljaidi, R. Bin Sulaiman, and A. A. Alshammari, "Brain tumor classification utilizing pixel distribution and spatial dependencies higher-order statistical measurements through explainable ML models," *Sci. Rep.*, vol. 14, no. 1, p. 25800, Oct. 2024, doi: 10.1038/s41598-024-74731-8.

